⑨ パーキンソン病初期（未治療患者）の治療（アルゴリズム参照）

- 現在用いられている治療ではADLや生命予後を改善させるが、ドパミン神経の変性を遅らせるエビデンスはく、治療を開始する際には症状の程度、日常生活の不自由さ、職業を勘案して開始する。
- ドパミン受容体作動薬で治療を開始した場合ジスキネシアの発現を遅らせるが精神症状の副作用が問題になる。そのため70歳から75歳以上の高齢者や認知症を合併している症例では精神症状の発症リスクを考慮してレボドパで治療を開始する。60歳代以下の症例は長期にわたって治療を続ける必要があるためドパミン受容体作動薬で治療開始する事が推奨されている。
- 症状を速やかに改善させる必要がある場合は有効性が高いレボドパで治療を開始する。レキップ®CR錠のデータでは、レボドパで治療されている症例にドパミン受容体作動薬を併用した場合はレボドパのみで治療した場合と比較してジスキネジアの発現を遅らせたため、レボドパで治療開始する事にあまり躊躇することはなく、ドパミン受容体作動薬を併用しながら治療する。

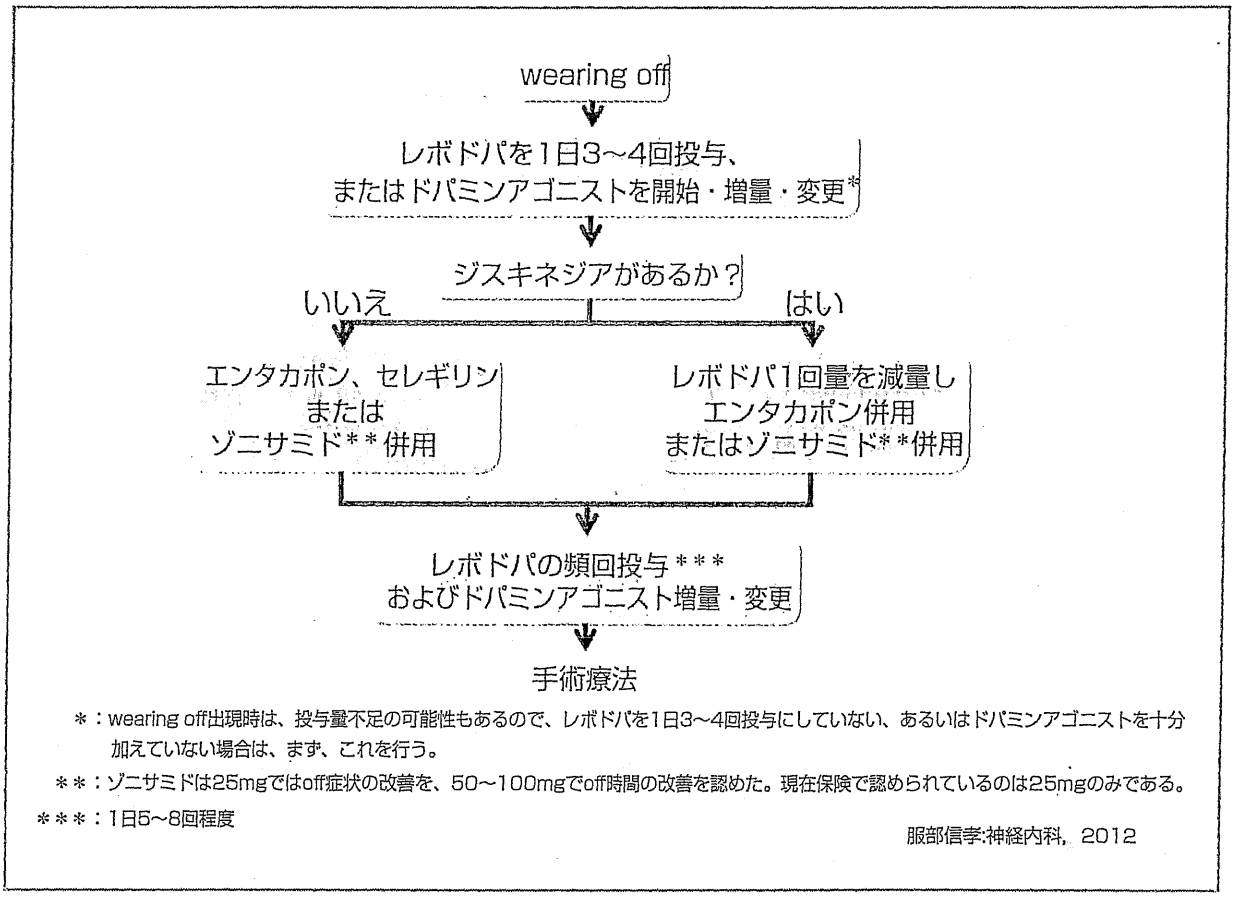

図3 Wearing offの治療アルゴリズム

⑩　ウェアリングオフの治療（アルゴリズム図参照）

- ウェアリングオフの治療はオフ時間の短縮と、オフ症状の改善の二つが重要である。
- コムタン®錠、ドパミン受容体作動薬はオフ時間の短縮およびオフ症状の改善効果がある。ドパミン受容体作動薬の種類や速崩錠、徐放錠、貼付剤など投与経路の差に関するエビデンスはない。
- エフピー®OD錠はオフ時間を短縮する。
- ノウリアスト®錠は困るジスキネジアを増やすことなくオン時間を延長させ、オフ時間を短縮する。
- トレリーフ®錠は50mg投与でオフ時間を短縮する。
- アポカイン®皮下注はオフ時に皮下注すると速やかにオフ症状を改善する。
- レボドパの頻回投与は良く行われる。しかしどの程度分割するべきか、食事との関係による血中濃度の変化、一回の至適投与量などに関するエビデンスは無く個々の症例に合わせて行う必要がある。
- 薬の調整で難しい場合は脳深部刺激療法を考慮する。ターゲットは視床下核か淡蒼球内節である。両者に関して効果は同等もしくは視床下核を刺激する方が運動症状に効果が高いとされている。視床下核の刺激では薬の量を減らすことができるが淡蒼球内節の刺激は精神症状の発現頻度が比較的少ない。

⑪　生活の支障となるpeak-dose dyskinesiaとoff-periodジストニア（早朝ジストニア）の治療アルゴリズム

- ジスキネジアにはオン時に生じるpeak dose dyskinesiaと薬の効果が切れかかるときもしくは立ち上がるときに生じるdiphasic dyskinesiaがある。
- Peak dose dyskinesiaの場合、患者本人が気にしていなければ特に治療する必要は無い。しかし日常生活に支障がある場合は以下のステップで治療する。①ジスキネジアを増悪させるようなエフピー®OD錠やコムタン®錠を併用している場合は中止する。②レボドパの1回量を減らし投与回数を増やす。③レボドパの1日量を減量する。オフ症状が悪化したりオン時の有効性が得られたりしない場合はドパミン受容体作動薬を併用する。④シンメトレル®錠を投与する。⑤調整が難しい場合は脳深部刺激療法を行う。
- Diphasic dyskinesiaの治療は確立された方法がなく困難である。下肢優位に出現し、しばしば痛みを伴うジストニアが出現するため、困る症状として訴

えることが多い。治療としてはジスキネジアに影響するコムタン®錠やエフピー®OD錠は中止する。オフ時間を減らすようにレボドパの1回量をそのまま、または減量して投与回数を増やして有効な場合があるが、むしろ一日中ジスキネジアが出現してしまうこともある。その場合はレボドパの１回量を増やして投与回数は減らしdiphasic dyskinesiaの出現を予測しやすくする。

- 脳深部刺激療法は視床下核を刺激する場合、薬剤の減量が可能となりジスキネジアを減らすことができる。淡蒼球内節を刺激する場合、薬剤は減量できないが直接にジスキネジアを止めることができる。

⑫ 幻覚、妄想の治療アルゴリズム

- 患者自身が幻覚として認識し、軽度である場合は治療する必要は無い。
- 薬剤で幻覚が引き起こされた場合は、直近に加えた薬剤を中止する。それでも改善しない場合は幻覚を引き起こしやすい抗コリン剤、シンメトレル®錠、エフピー®OD錠を中止する。次いでトレリーフ®錠、ドパミン受容体作動薬、コムタン®錠を中止し、レボドパ製剤のみで加療する。
- 幻覚が強い場合は抑肝散、セロクエル®錠を投与する。コリンエステラーゼ阻害薬も幻視、幻覚に有効であるが興奮性が増悪することがある。現在コリンエステラーゼ阻害剤はアリセプト®D錠、レミニール®錠、イクセロン®パッチがある。

⑬ すくみ足、睡眠障害の治療についてはアルゴリズムの表参照。

おわりに

PDの治療選択は増えており、匙加減的治療が益々求められるようなったといえる。脳深部刺激療法もあり、テーラーメイド的な治療が可能となっている。積極的な治療を施すことでPDのADLは間違いなく改善している。一方、認知症など非運動症状がQOLの大きな因子であることが分かっており、今後進行を抑える治療の実現が不可欠と考える。本解説が日常の処方に少しでも役に立つことを願っている。

文献

1．Farrer MJ. Genetics of Parkinson disease: paradigm shifts and future

prospects. Nat Rev Genet. 2006 Apr;7 (4) :306-18.
2. Proukakis C, Dudzik CG, Brier T, MacKay DS, Cooper JM, Millhauser GL, et al. A novel alpha-synuclein missense mutation in Parkinson disease. Neurology. 2013 Mar 12;80 (11) :1062-4.
3. Lesage S, Anheim M, Letournel F, Bousset L, Honore A, Rozas N, et al. G51D alpha-synuclein mutation causes a novel parkinsonian-pyramidal syndrome. Ann Neurol. 2013 Mar 22.
4. Nishioka K, Ross OA, Ishii K, Kachergus JM, Ishiwata K, Kitagawa M, et al. Expanding the clinical phenotype of SNCA duplication carriers. Mov Disord. 2009 Sep 15;24 (12) :1811-9.
5. Kitada T, Asakawa S, Hattori N, Matsumine H, Yamamura Y, Minoshima S, et al. Mutations in the parkin gene cause autosomal recessive juvenile parkinsonism. Nature. 1998 Apr 9;392 (6676) :605-8.
6. Corti O, Lesage S, Brice A. What genetics tells us about the causes and mechanisms of Parkinson's disease. Physiol Rev. 2011 Oct;91 (4) :1161-218.
7. Valente EM, Abou-Sleiman PM, Caputo V, et al. Hereditary early-onset Parkinson's disease caused by mutations in PINK1. Science 2004;304:1158-60
8. Hatano Y, Li Y, Sato K, et al. Novel PINK1 mutations in early-onset parkinsonism. Ann Neurol 2004;56:424-7
9. Kilarski LL, Pearson JP, Newsway V, et al. Systematic review and UK-based study of PARK2 (parkin) , PINK1, PARK7 (DJ-1) and LRRK2 in early-onset Parkinson's disease. Mov Disord 2012;27:1522-9
10. Ibanez P, Lesage S, Lohmann E, et al. Mutational analysis of the PINK1 gene in early-onset parkinsonism in Europe and North Africa. Brain 2006;129:686-94
11. Gandhi S, Muqit MM, Stanyer L, et al. PINK1 protein in normal human brain and Parkinson's disease. Brain 2006;129:1720-31
12. Samaranch L, Lorenzo-Betancor O, Arbelo JM, et al. PINK1-linked parkinsonism is associated with Lewy body pathology. Brain 2010;133:1128-42
13. Matsuda N, Sato S, Shiba K, et al. PINK1 stabilized by mitochondrial

depolarization recruits Parkin to damaged mitochondria and activates latent Parkin for mitophagy. J Cell Biol 2010;189:211-21

14. Grenier K, McLelland GL, Fon EA Parkin- and PINK1-Dependent Mitophagy in Neurons: Will the Real Pathway Please Stand Up? Front Neurol 2013;4:100
15. Nukada H, Kowa H, Saitoh T, et al. A big family of paralysis agitans. Rinsho Sinkeigaku. 1978;18:627-34
16. Funayama M, Hasegawa K, Kowa H, Saito M, Tsuji S, Obata F. A new locus for Parkinson's disease (PARK8) maps to chromosome 12p11.2-q13.1. Ann Neurol. 2002 Mar;51 (3) :296-301.
17. Zimprich A, Biskup S, Leitner P, Lichtner P, Farrer M, Lincoln S, et al. Mutations in LRRK2 cause autosomal-dominant parkinsonism with pleomorphic pathology. Neuron. 2004 Nov 18;44 (4) :601-7.
18. Paisán-Ruíz C, Jain S, Evans EW, et al. Cloning of the gene containing mutations that cause PARK8-linked Parkinson's disease. Neuron 2004;44:595-600.
19. Funayama M, Hasegawa K, Ohta E, et al. An LRRK2 mutation as a cause for the parkinsonism in the original PARK8 family. Ann Neurol 2005;57:918-21
20. Nichols WC, Pankratz N, Hernandez D, et al. Genetic screening for a single common LRRK2 mutation in familial Parkinson's disease. Lancet 2005;365:410-12
21. Di Fonzo A, Rohe CF, Ferreira J, et al. A frequent LRRK2 gene mutation associated with autosomal dominant Parkinson's disease. Lancet 2005;365:412-15.
22. Gilks WP, Abou-Sleiman PM, Gandhi S, et al. A common LRRK2 mutation in idiopathic Parkinson's disease. Lancet 2005;365:415-16
23. Lesage S, Durr A, Tazir M, et al. LRRK2 G2019S as a cause of Parkinson's disease in North African Arabs. N Engl J Med 2006 Jan 26;354:422-23
24. Kachergus J, Mata IF, Hulihan M, et al. Identification of a novel LRRK2 mutation linked to autosomal dominant parkinsonism: Evidence of a common founder across European populations. Am J Hum Genet

2005;76:672-80

25. Funayama M, Li Y, Tomiyama H, et al. Leucine-Rich Repeat kinase 2 G2385R variant is a risk factor for Parkinson disease in Asian population. Neuroreport 2007;18:273-75
26. 長谷川一子. PARK8-パーキンソニズムについて. 神経内科 2006;65:121-27

FEBS Letters 587 (2013) 1316–1325

FEBS Letters

journal homepage: www.FEBSLetters.org

ATP13A2 deficiency induces a decrease in cathepsin D activity, fingerprint-like inclusion body formation, and selective degeneration of dopaminergic neurons

Hideaki Matsui [a,g,1,2], Fumiaki Sato [b,g,1,3], Shigeto Sato [b,g], Masato Koike [f], Yosuke Taruno [a,g], Shinji Saiki [b,g], Manabu Funayama [d,g], Hidefumi Ito [a,g], Yoshihito Taniguchi [c,g,4], Norihito Uemura [a,g], Atsushi Toyoda [e,6], Yoshiyuki Sakaki [e,5], Shunichi Takeda [c,g], Yasuo Uchiyama [f], Nobutaka Hattori [b,g,*], Ryosuke Takahashi [a,g,*]

[a] Department of Neurology, Kyoto University Graduate School of Medicine, Kyoto 606-8507, Japan
[b] Department of Neurology, Juntendo University, School of Medicine, 2-1-1 Hongo, Bunkyo-ku, Tokyo 113-8421, Japan
[c] Department of Radiation Genetics, Kyoto University Graduate School of Medicine, Kyoto 606-8501, Japan
[d] Research Institute for Diseases of Old Age, Juntendo University, School of Medicine, 2-1-1 Hongo, Bunkyo-ku, Tokyo 113-8421, Japan
[e] RIKEN Genomic Sciences Center, Yokohama 230-0045, Japan
[f] Department of Cell Biology and Neuroscience, Juntendo University, School of Medicine, 2-1-1 Hongo, Bunkyo-ku, Tokyo 113-8421, Japan
[g] Core Research for Evolutional Science and Technology (CREST), Japan Science and Technology Agency, Kawaguchi 332-0012, Japan

ARTICLE INFO

Article history:
Received 5 January 2013
Revised 22 February 2013
Accepted 25 February 2013
Available online 13 March 2013

Edited by Barry Halliwell

Keywords:
Parkinson's disease
Medaka fish
ATP13A2
Lysosome

ABSTRACT

Kufor-Rakeb syndrome (KRS) was originally described as an autosomal recessive form of early-onset parkinsonism with pyramidal degeneration and dementia. *ATP13A2* was identified as the causative gene in KRS. *ATP13A2* encodes the ATP13A2 protein, which is a lysosomal type5 P-type ATPase, and ATP13A2 mutations are linked to autosomal recessive familial parkinsonism.

Here, we report that normal ATP13A2 localizes in the lysosome, whereas disease-associated variants remain in the endoplasmic reticulum. Cathepsin D activity was decreased in ATP13A2-knockdown cells that displayed lysosome-like bodies characterized by fingerprint-like structures. Furthermore, an atp13a2 mutation in medaka fish resulted in dopaminergic neuronal death, decreased cathepsin D activity, and fingerprint-like structures in the brain. Based on these results, lysosome abnormality is very likely to be the primary cause of KRS/PARK9.

1. Introduction

Parkinson's disease (PD) is one of the most common movement disorders, and it is caused by loss of dopaminergic neurons. The molecular mechanisms underlying neuronal degeneration in PD remain unknown; however, it is now clear that genetic factors heavily contribute to the pathogenesis of this disease [1]. In approximately 10% of patients with clinical features of PD, the disease state has a strict familial etiology.

PARK9-linked PD is an autosomal recessive early-onset disorder that is characterized by levodopa-responsive parkinsonism, supranuclear gaze palsy, pyramidal signs, and dementia; this condition is also called Kufor-Rakeb syndrome (KRS), being named for a consanguineous Jordanian family containing four members with this disorder [2]. Recently, *ATP13A2* was identified as the causative gene for KRS/PARK9. The *ATP13A2* gene comprises 29 exons that encode a lysosomal type 5 P-type ATPase with 10 transmembrane domains [3]. Thus far, eight mutations have been reported in just five families and in two additional unrelated patients, and no neuropathological examination of an autopsy case has been documented [3–8]. The function of the ATP13A2 protein remains largely unknown, but it is supposed that ATP13A2 might participate in autophagic protein degradation via the lysosomal pathway [9].

Here, we established and analyzed a cell culture model of ATP13A2 knockdown and Atp13a2 mutant medaka fish to elucidate the mechanisms underlying PARK9-associated pathology.

* Corresponding authors.
E-mail addresses: nhattori@juntendo.ac.jp (N. Hattori), ryosuket@kuhp.kyoto-u.ac.jp (R. Takahashi).
[1] These authors contributed equally to this work.
[2] Current address: Department of Cell Physiology, Zoological Institute, Technical University Braunschweig, Spielmannstrasse 8, Braunschweig 38106, Germany.
[3] Current address: Department of Clinical Chemistry, Hoshi University School of Pharmacy and Pharmaceutical Sciences, 2-4-41 Ebara, Shinagawa-ku, Tokyo 142-8501, Japan.
[4] Current address: Department of Preventive Medicine and Public Health, School of Medicine, Keio University, 35, Shinano-cho, Shinjuku-ku, Tokyo 160-8582, Japan.
[5] Current address: Toyohashi University of Technology, 1-1, Hibarigaoka, Tenpaku-cho, Toyohashi, Aichi 441-8580, Japan.
[6] Current address: Comparative Genomics Laboratory, National Institute of Genetics, Yata 1111, Mishima, Shizuoka 411-8540, Japan.

0014-5793/$36.00
http://dx.doi.org/10.1016/j.febslet.2013.02.046

Both the cultured cells and the mutant fish exhibited decreased cathepsin D enzymatic activity, fingerprint-like inclusion body formation, and neuronal death. These findings indicated that abnormalities in lysosome function are the primary defect in KRS/PARK9.

2. Results

2.1. Wild-type ATP13A2 localizes to the lysosome, but some disease-relevant variants localize to the endoplasmic reticulum

To investigate the subcellular localization of ATP13A2, we used an anti-V5 antibody and antibodies that recognize several markers of intracellular organelles to double label SH-SY5Y cells that stably expressed wild-type ATP13A2 fused to the V5 epitope (WT-V5). The WT-V5 signal largely colocalized with the signal of cathepsin D, a lysosomal aspartic protease (Fig. 1A and S1). Additionally, WT-V5 partially overlapped with makers of the Golgi apparatus (GM130), the late endosome (Rab7) and the autophagosome (LC3B), but not with the markers of the endoplasmic reticulum (ER) (GRP78), the mitochondria (Tom20), the early endosome (EEA1 and Rab5), or the exocytotic vesicles (Rab3 and 4) (Fig. 1A, B and S1). GFP signals in SH-SY5Y cells that stably expressed GFP-tagged wild-type ATP13A2 (GFP-WT) strongly colocalized with either of two lysosomal membrane proteins, Lamp2 (Fig. 1A and S1) or Lamp1 (data not shown). Furthermore, immunoelectron microscopy using ultrathin cryosections of GFP-WT SH-SY5Y cells confirmed that gold particles labeling GFP-WT (arrow head: 10 nm gold) and those labeling Lamp1 (arrow: 5 nm gold) co-localized on the lysosomal membrane (Fig. 1C). These data indicated that ATP13A2 is a resident protein of the lysosomal membrane.

Thus far, eight disease-associated mutations have been identified in the *ATP13A2* gene, including one that we described initially [3–8]. To determine whether the mutant proteins were mislocalized and whether any such mislocalization has etiological importance, we assessed the subcellular localization of five pathogenic protein variants (Fig. 2A). These mutants were each tagged with a V5 epitope and then transiently transfected into SH-SY5Y cells. To, first, characterize the subcellular distribution of KRS mutants, we separated cell homogenates by Percoll density gradient centrifugation. This Percoll gradient system separates dense lysosomes (near bottom) from lighter particles such as ER. We found that WT-V5 was mainly co-fractionated with lysosomal component (Lamp1 and cathepsin D; Fraction No. 13–16, Fig. 2B). However, an ATP13A2 variant that lacks exon 13 (1306 + 5G→A) but maintains the reading frame was co-fractionated not with lysosomal proteins but with GRP78 (Fraction No. 2–8, Fig. 2B): this finding indicated that the protein variant accumulated in the ER. Some other ATP13A2 pathogenic variants (F182L and G504R) also accumulated in the ER in a manner similar to the 1306 + 5G→A variant. In contrast, the other two pathogenic variants (T12M and G533R) were co-fractionated with lysosomal components, as was the WT protein. To, further, confirm the subcellular localization, we carried out double fluorescence immunocytochemistry of permeabilized SH-SY5Y cells by staining KRS mutants (V5), the ER marker (GRP78), the lysosomal marker (cathepsin D) and the mitochondria marker (Tom20). Along with immunoblotting of Percoll density gradient fractionation, immunofluorescence studies showed 1306 + 5G→A mutant, F182L and G504R colocalized with GRP78 and the other two variants (T12M and G533R) colocalized with cathepsin D as already reported [10–14] (Fig. 2C and S1). The expression levels of ATP13A2 mutant proteins that accumulated in the ER (F182L, G504R, and 1306 + 5G→A) were lower than that of the WT protein and MG132 inhibited degradation of the all ATP13A2 variants as well as that of the WT protein (Fig. 2D).

2.2. Stable knockdown of ATP13A2 induces cathepsin D deficiency and structures that resemble neuronal ceroid-lipofuscinosis deposits

To assess whether the loss of normal ATP13A2 functions has a causal role in PD pathogenesis, the expression of endogenous ATP13A2 was suppressed in SH-SY5Y cells by gene knockdown. By using antibodies that we generated (Fig. 3A), we showed that endogenous ATP13A2 protein levels in SH-SY5Y cells that stably expressed ATP13A2 shRNA (ATP13A2shRNA-1 or -2) were efficiently suppressed (Fig. 3B). Water soluble Tetrazolium salts (WST)-8 assay demonstrated that ATP13A2 knockdown caused a significant reduction of the cell growth in SH-SY5Y cells (Fig. 3B). Next, we determined the distribution and the morphology of lysosomes in SH-SY5Y cells subjected to ATP13A2 knockdown. Immunostaining of cathepsin D and Lamp2 indicated that ATP13A2 deficiency led to the assembly of lysosomes in the perinuclear region and decreased cathepsin D staining (Fig. S2). The protein amount of full length (52-kDa), immature (44-kDa) and mature (32-kDa) forms of cathepsin D of the cells expressing ATP13A2 shRNAs were all decreased together with the enzyme activity (Fig. 3C). To show the reduction of cathepsin D activity was indeed induced by the reduction of ATP13A2, not by the non-specific effect of shRNA, we generated shRNA-resistant species of ATP13A2. SH-SY5Y cells stably expressing ATP13A2 shRNAs that were transfected with shRNA resistant ATP13A2 showed comparable cathepsin D activity to the controls (Fig. S3A). The activity and amount of mature forms (25-kDa) of cathepsin B and L were also decreased in the knockdown cells line by ATP13A2 shRNA-1, but not shRNA-2, suggesting that the loss of ATP13A2 principally gives rise to the reduction of cathepsin D (Fig. 3C). Finally, analysis via transmission electron microscopy revealed that lysosome-like bodies became more numerous in ATP13A2 shRNAs expressing cells and that very immense high density structure appeared adjacent to the nucleus in these cells (Fig. 3D: a–h). High-magnification images revealed that the abnormal structures in these cells included fingerprint profiles-like structure (Fig. 3D: e), and these structures were very similar to the structure of the neurons in mice lacking cathepsin D [15]. The levels of LC3-II, autophagosome marker, in shRNA-1 transfected cells were increased (Fig. 3E) and p62 a substrate of autophagic degradation, was accumulated in both of the shRNA expressing lines (Fig. S3B), suggesting that an appearance of abnormal structure induced by ATP13A2 deficiency might be involved with impaired lysosomal proteolysis. Taken together, these findings indicated that loss of ATP13A2 led to lysosomal pathology and, more specifically, a reduction in cathepsin D activity.

2.3. Generation of an Atp13a2 mutant medaka fish

Next, we generated and evaluated medaka fish with an Atp13a2 mutation to investigate the mechanism of KRS/PARK9-associated neurodgeneration in vivo. The draft of the medaka genome contains only one identifiable ortholog of the human *ATP13A2* gene. We cloned the medaka *atp13a2* gene by RT-PCR and RACE, and it encoded a protein consisting of 1159 amino acids. The amino-acid sequence showed 51.3% homology to human ATP13A2 protein (Fig. S4A). To characterize medaka *atp13a2* expression, we used in situ hybridization to visualize medaka *atp13a2* mRNA. No signal was observed with the sense RNA probe. However, the anti-sense RNA probe resulted in diffuse signals in the gray matter of medaka brain (Fig. 4A). The telencephalon and diencephalon that contain the putative striatum and many dopaminergic neurons, respectively, were intensely labeled by the anti-sense probe. The optic tectum was also intensely labeled, but the hindbrain and spinal cord were scarcely labeled (Fig. 4A).

We then used TILLING (Targeting Induced Local Lesions In Genomes) method to generate an Atp13a2 mutant fish [16]. We

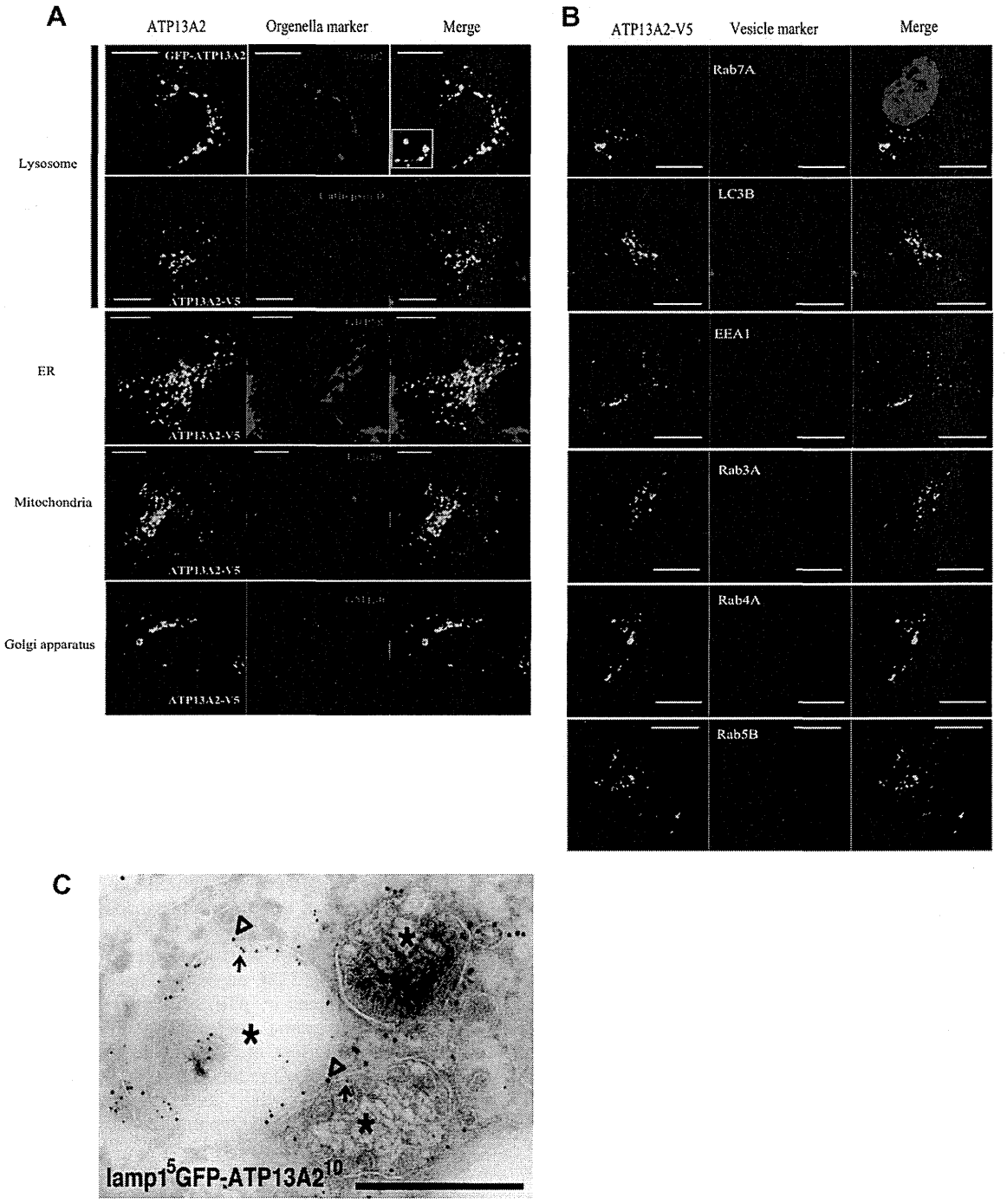

Fig. 1. Wild-type ATP13A2 localizes at lysosomal membranes. (A and B) WT-V5 and GFP-WT fusion proteins consistently co-localizes with Lamp2 and cathepsin D. Additionally, WT-V5 partially overlapped with GM130, Rab7 and LC3B. (Scale bar; 10 μm). (C) Immunoelectron microscopy using ultrathin cryosections. Double immunostaining of GFP-ATP13A2 (gold particles, 10 nm in diameter (open arrowheads)) and Lamp1 (gold particles, 5 nm in diameter (arrows)). Both types of immuno-gold label clearly localizes along the membranes around lysosomes (asterisks). (Scale bar; 0.5 μm).

sequenced the genomes of 5771 samples obtained from our ENU-mutagenized medaka library, and identified one mutation "IVS13, T-C, +2" that resulted in an aberrant splice donor site (Fig. 4B). The IVS13, T-C, +2 mutant from this strain was subjected to six sequential backcrosses to generate the mutant used in the following experiments. A cross between heterozygous "IVS13, T-C, +2" mutant pair resulted in wild-type fish (WT/WT), heterozygous mutants (WT/mt), and homozygous mutants (mt/mt) in Mendelian ratios. RT-PCR analysis revealed an abnormal splice variant in the WT/mt and mt/mt medaka (Fig. 4C), and the sequence of these PCR products indicated that exon 13 was skipped in the mutant mRNAs (Fig. 4D). Surprisingly, this abnormal splicing pattern was almost identical to that in the human KRS/PARK9 patient [3], in which the 111-bp exon 13 is skipped (Fig. S4B). Real-time PCR showed a marked reduction (17.8%) in the normal *atp13a2* mRNA in the mt/mt medaka brain (Fig. 4E). We therefore concluded that we had succeeded in identifying an Atp13a2 mutant in medaka, and this mutation was similar to a pathogenic KRS/PARK9 mutation in human.

Atp13a2 mutant medaka fish grew normally during early development without any obvious morphological abnormalities.

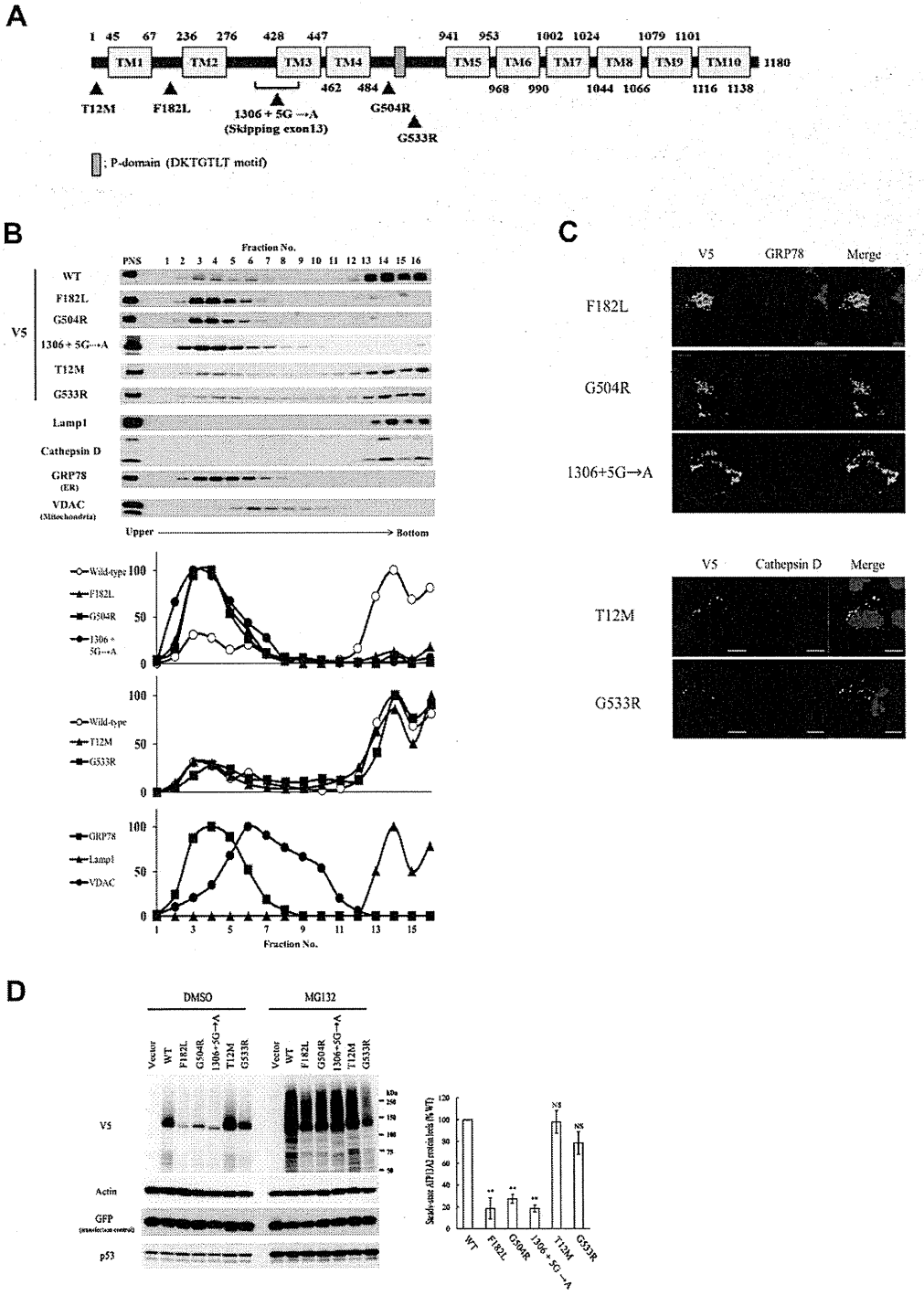

Fig. 2. Characterization of subcellular localization of KRS mutants. (A) Schematic diagram of disease-relevant mutants of ATP13A2 used in this study. (B) Percoll gradient fractionation of ATP13A2 protein. The graphs indicate densitometry of bands. This Percoll gradient system separates dense lysosomes (near bottom, Fraction 13–16) from lighter particles such as ER (Fraction 2–8). (C) Double immunofluorescence studies for KRS mutants. Colocalization of T12M or G533R with cathepsin D, a lysosomal protein, is observed. Other mutants localizes with GRP78, a resident ER chaperone protein. (D) Protein blot analysis of ATP13A2 WT and mutant V5-tagged constructs in transiently transfected SH-SY5Y cells. GFP was co-transfected with the ATP13A2s as a transfection control. The proteasome inhibitor MG132 (10 μM) stabilizes PARK9 mutants after 24 h. The antibody against p53, whose degradation is known to dependent to proteasome, is used as a control for MG132 treatment. Densitometry analysis indicates the steady state protein levels of each variant. Data are represented as percent of WT. Error bars, S.E.M. $n = 3$. $^{**}P < 0.01$ vs WT.

Remarkably, the mt/mt medaka fish showed a significant reduction of the life span relative to WT/WT and to WT/mt fish (Fig. 4F). The body weight of mt/mt fish was normal (Fig. 4G). We examined the internal organs including brains of the dead mt/mt fish, but we could not identify a specific reason for the shorter lifespan of mt/mt medaka fish. We next quantified spontaneous swimming movement in mt/mt medaka fish. At 4 months, mt/mt fish exhibited a mild locomotor increase with significant differences reported only in swimming duration whereas distance and velocity are normal. All the genotypes showed comparable movement at 12 months, irrespective of *atp13a2* genotype (Fig. 4H).

Collectively, we generated *atp13a2* mutant medaka fish carrying almost identical mutation to human KRS/PARK9 patient. The homozygous mutant fish grew normally, but relative to wild-type and heterozygous animals, these mutants exhibited more spontaneous swimming movement at 4 months and had a shorter life span.

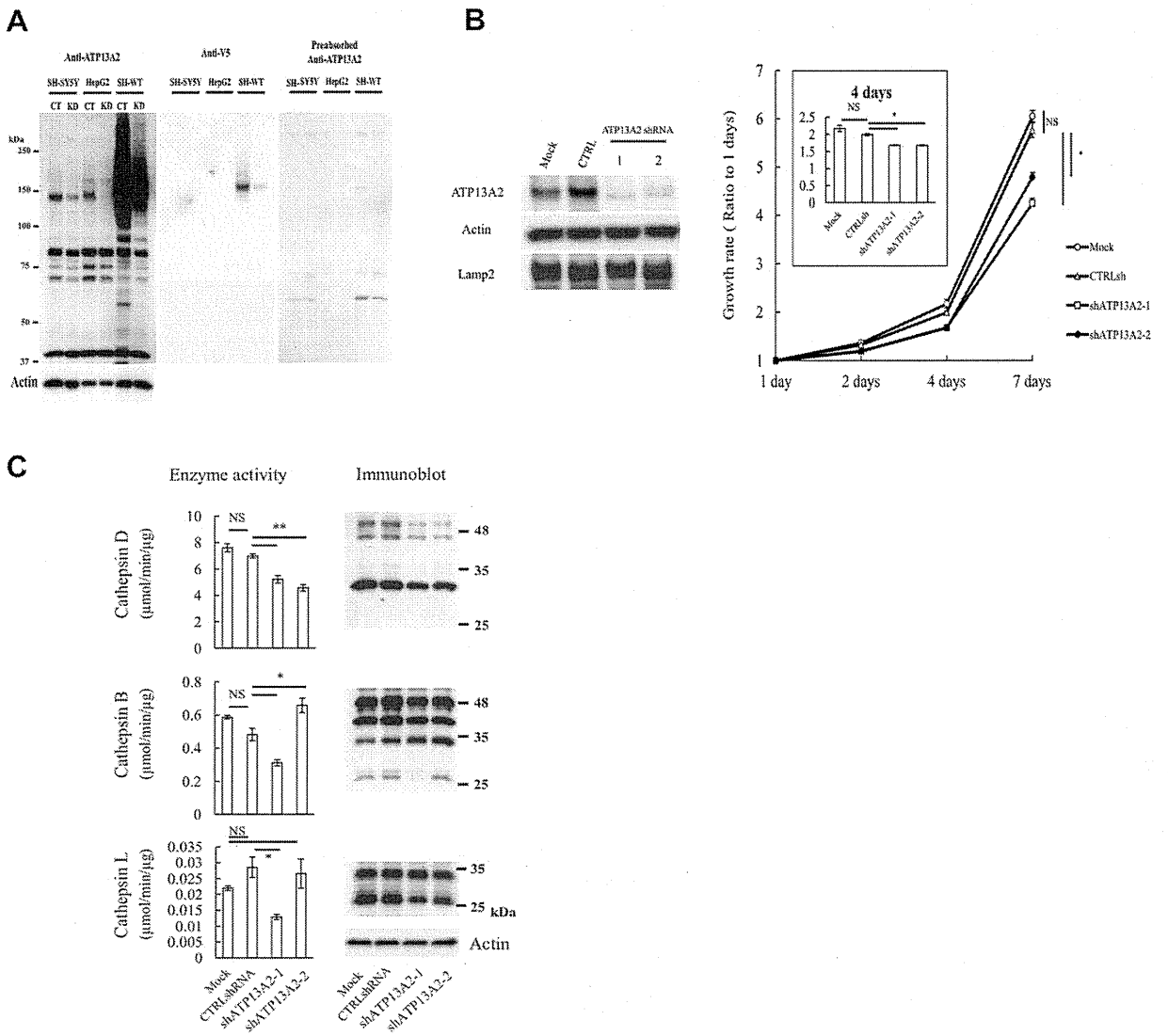

Fig. 3. Suppression of ATP13A2 leads to cathepsin D deficiency and accumulation of fingerprint-like structures in SH-SY5Y cells. (A) Immunoblotting with anti-ATP13A2 antibody (left panel), anti-V5 antibody (middle panel) and anti-ATP13A2 antibody (preabsorbed) (right panel) shows the ATP13A2 expression levels of SH-SY5Y cells, HepG2 cells and SH-SY5Y cells stably expressing WT (SH-WT). Cells are transfected with negative control (CT) or ATP13A2 siRNA (KD) for 72 h. (B) Immunoblotting using anti-ATP13A2 antibody and cell growth assay of SH-SY5Y cell lines stably expressing shRNA against human ATP13A2. The graph shows the growth rate of cells. Data are the means of triplicate experiments. Error bars, S.E.M. $^{*}P < 0.05$. (C) Measurement of cathepsin D, B and L activity and protein level in the extracts from ATP13A2-knockdown SH-SY5Y cells. Enzyme activity assays were performed in three independent experiments. Error bars, S.E.M. $^{*}P < 0.05$. $^{**}P < 0.01$. (D) Electron microscopic examination of SH-SY5Y cells that stably express shATP13A2-1 or shATP13A2-2. The diminished ATP13A2 expression induces lysosome-like bodies that contain granular deposits and fingerprint-like structure. Boxed areas (d) are shown enlarged in the left (e). (E) Evaluation of LC3 accumulation using anti-LC3B antibody in SH-SY5Y cell lines stably expressing shATP13A2 (each 3 clones). $^{**}P < 0.01$.

2.4. Neuropathology of Atp13a2 mutant medaka fish

Selective and progressive loss of dopaminergic/noradrenergic cells constitutes the characteristic pathology of human PD patients. Having previously identified TH-positive (TH+) dopaminergic neurons and noradrenergic neurons in the medaka brain [17], we could examine histologically these TH+ neurons in the brain tissue of *atp13a2* mutants. At 4 months, the number of TH+ neurons did not differ significantly among mt/mt, mt/WT, and WT/WT fish. However at 8 and 12 months, the number of TH+ neurons in the middle diencephalon and the density of TH+ fibers in the telencephalon were lower in the mt/mt medaka than in mt/WT or in WT/WT fish (Fig. 5A). The mt/mt medaka fish at these stages also had fewer noradrenergic neurons in the medulla oblongata than did mt/WT or WT/WT fish (Fig. 5A). The reduction of TH+ neurons was not robust but age-dependent and progressive. Additionally, we examined tryptophan hydroxylase and serotonin levels via immunohistochemistry; neither the number of tryptophan hydroxylase positive neurons in the raphe nor the intensity of serotonin signals in the diencephalon differed significantly among all the genotypes (Fig. 5A). Although no TUNEL-positive dopaminergic neuron was observed in the WT/WT brains, a few TUNEL/TH double positive neurons were detected in the mt/mt brains (Fig. 5B). To exclude the possibility of developmental disorder of the dopaminergic neurons, we also counted the TH+ neurons in the middle diencephalon at 1 month. At this larval stage, mt/mt fish showed comparable number of dopaminergic neurons to WT/WT fish (Fig. S5) indicating the loss of dopaminergic neurons seen at 8 and 12 months was indeed late-onset phenotype. Next, we measured the amount of dopamine, noradrenaline, and serotonin in whole-brain samples from mutant fish at 4 and 12 months. The amount of dopamine in the brain samples from mt/mt medaka

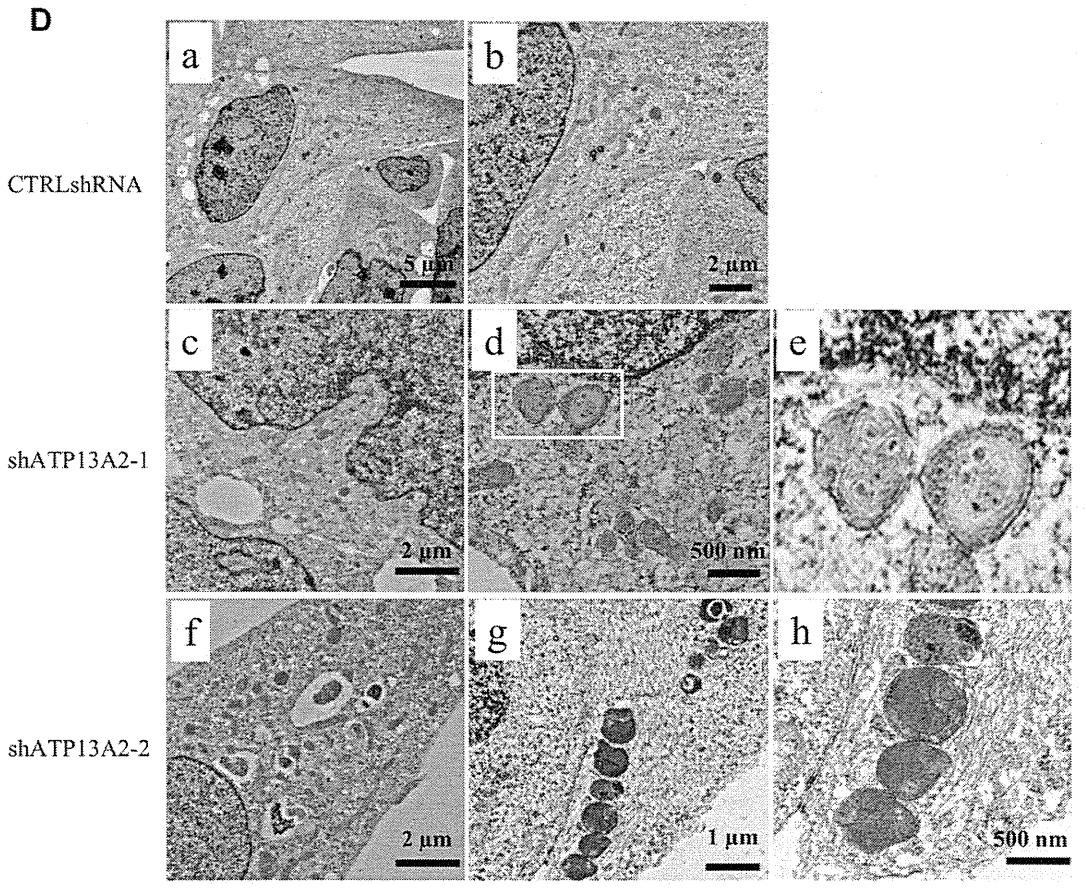

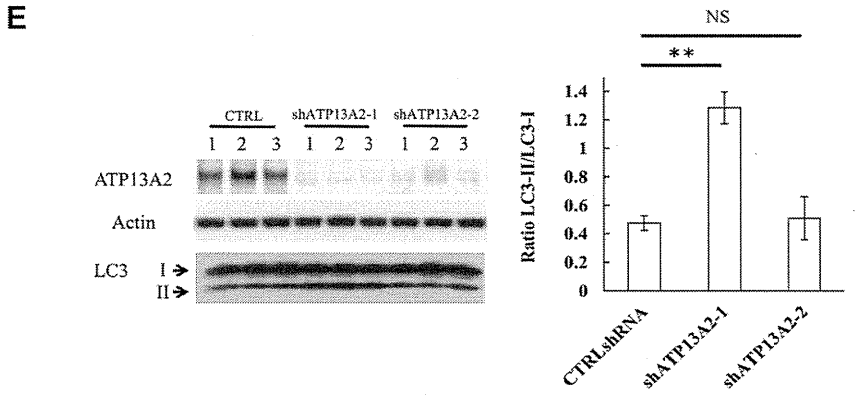

Fig. 3. (*continued*)

was comparable to that in the WT/WT or the WT/mt at 4 months, but lower than that in the WT/WT or the WT/mt at 12 months (Fig. 5C, upper). The noradrenaline in mt/mt medaka brain samples also tended to be lower at 12 months, but the differences were not statistically significant (Fig. 5C, middle). The amount of serotonin in whole-brain samples did not differ significantly among the genotypes (Fig. 5C, lower). Taken together, these findings indicated that *atp13a2* homozygous mutant medaka fish showed selective and progressive loss of dopaminergic/noradrenergic neurons, and such loss is a typical feature of human PD.

To examine in further detail the pathology associated with the *apt13a2* mutation, middle diencephalon samples from mt/mt, mt/WT, and WT/WT animals were analyzed via transmission electron microscopy as described previously [18]. Structures resembling fingerprints-profile, like those seen in ATP13A2-knockdown SH-SY5Y cells, were observed in thin sections taken from each mt/mt brain examined (Fig. 5D). However, these structures were not observed in the sections taken from WT/WT or WT/mt medaka brain samples. Fingerprint-profiles have been observed in cathepsin D-deficient mice [15] and in human patients with neuronal ceroid lipofuscinosis [19–21], and these structures are thought to indicate an autophagy/lysosome disorder. We used western blots to measure the amount of cathepsin D protein in brain tissue samples, and we found that mt/mt fish had less cathepsin D protein than did mt/WT or WT/WT fish (Fig. 5E and S6). We also showed that mt/mt medaka brain tissue, like the ATP13A2-knockdown cells, exhibited a significant reduction in cathepsin D activity (Fig. 5E). However, cathepsin K activity, cathepsin H activity, and proteasome activity were not affected by the *atp13a2* mutation (Fig. 5E), indicating the dysfunction of lysosomal enzymes was relatively specific to cathepsin D. Alpha-synuclein accumulation is one of the specific characters of idiopathic PD patients, Thus, we

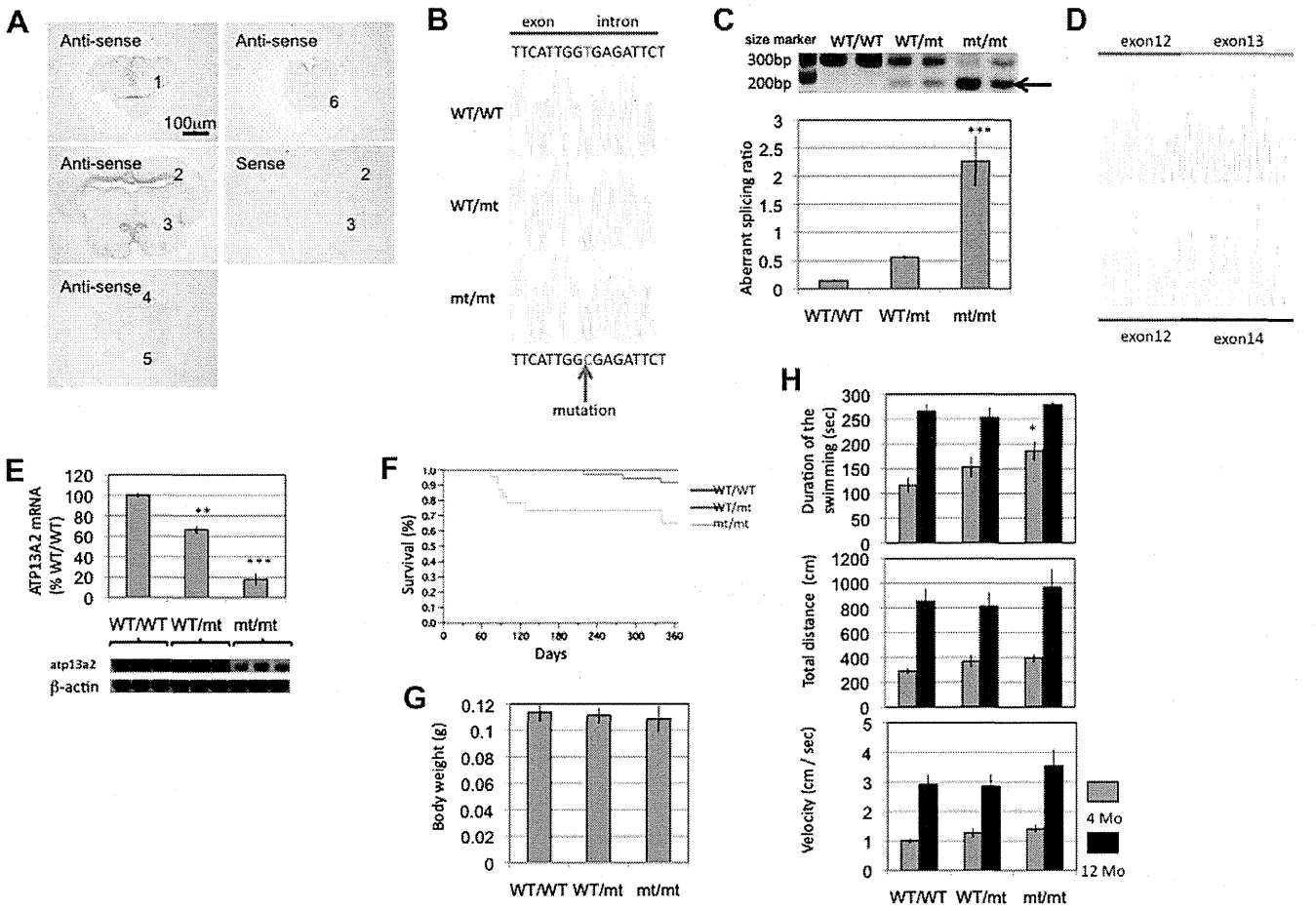

Fig. 4. Generation of Atp13a2 mutant medaka. (A) In situ hybridization of medaka *atp13a2* mRNA. Anti-sense signals and sense control of *Kyoto-Cab* medaka brain (12 months). 1: telencephalon, 2: optic tectum, 3: diencephalon, 4: cerebellum, 5: medulla oblongata, 6: spinal cord. (B) Sequence data for each genotype. A = green, T = red, G = black, and C = blue. The red arrow indicates the mutation site. This T to C mutation in the genomic sequence disrupts a splice donor site. (C) RT-PCR amplification of *atp13a2* mRNA from each genotype. WT/WT medaka show single band, whereas WT/mt and mt/mt medaka have an additional shorter band (arrow). bp: Base pairs. The graph indicates densitometric ratio of the shorter product/normal product. ***$P < 0.001$ vs. WT/WT and $P < 0.01$ vs. WT/mt. $n = 4$ for each genotype. Error bars, S.E.M. (D) Sequence of the PCR products. The upper band indicates the normal splicing product and the lower band is the abnormal splicing product. Exon 13 skipping occurrs in the Atp13a2 mutant medaka. (E) Real-time PCR of normal *atp13a2* mRNA. **: $P < 0.01$ vs. WT/WT, ***: $P < 0.001$ vs. WT/WT and WT/mt. $n = 3$ for each genotype. Error bars, S.E.M. (F) Survival curves of each genotype. The end point is the death of each medaka or day 365. The results show mild but significant shortening of the life span in mt/mt medaka ($P < 0.001$) ($n = 23$), relative to that in WT/WT ($n = 25$) or WT/mt ($n = 37$). Death before 1 month stage was not counted. (G) Body weight of Atp13a2 mutant medaka at 12 months. No significant differences were seen ($n = 20$ for each group). Error bars, S.E.M. (H) Duration of swimming, total swimming distance and swimming velocity during spontaneous swimming behavior of Atp13a2 mutant medaka ($n = 15$ for each group). *$P < 0.05$ vs. WT/WT. Error bars, S.E.M.

analyzed the alpha-synuclein status in our cell line and medaka models. However, we could not demonstrate consistent and significant differences between ATP13A2-deficient models and controls (Figs. S3 and S7), and these findings indicated that alpha-synuclein accumulation might not be the causative roles of KRS/PARK9.

In sum, *atp13a2* homozygous mutant medaka exhibited dopaminergic neurodegeneration, a deficiency of cathepsin D, and abnormal lysosome-related structures in the brain.

3. Discussion

Findings from previous studies clearly indicate that PARK gene products associate with each other via protein degradation pathways including the autophagy–lysosome system. Indeed, dysfunction of protein degradation has emerged as an important contributor to nigral neuronal death in PD. Presence of Lewy bodies is strong evidence of impaired protein degradation in PD. Lewy bodies consist of aggregated proteins, and alpha-synuclein is a major component of these structures [22]. Thus aggregation of alpha-synuclein has emerged as one of the most important processes in nigral degeneration in PD. Although soluble alpha-synuclein is degraded both during autophagy and by the proteasome, aggregated alpha-synuclein is degraded and cleared mainly via the autophagy–lysosome pathway [23]. Other PARK gene products, specifically Parkin and PINK1, work together to clear damaged mitochondria from cells via mitochondria-specific autophagy called mitophagy [24]. Furthermore, ATP13A2 mainly localizes to lysosomes, as we and other groups demonstrated [3,10–14,25]. Recently, mutations in the gene encoding glucocerebrosidase (GBA), a lysosomal enzyme, have been shown to be significant genetic risk factors for PD [26]. These observations indicate that lysosomal function is important for the maintenance of dopamine neurons, and they led us to investigate the function of ATP13A2 in the pathophysiology of KRS/PARK9.

ATP13A2 deficiency resulted in an abnormal aggregation of lysosomes at perinuclear site. Furthermore, these accumulated vesicles were enlarged, as previously reported [27]. Moreover, we found evidence of lysosomal dysfunction in that cathepsin D activity was, specifically, reduced in ATP13A2-knockdown cells. Cathepsin D is a ubiquitously expressed lysosomal protease that is involved in proteolytic degradation, cell invasion, and apoptosis. Cathepsin D deficiencies cause neuronal ceroid lipofuscinosis, a

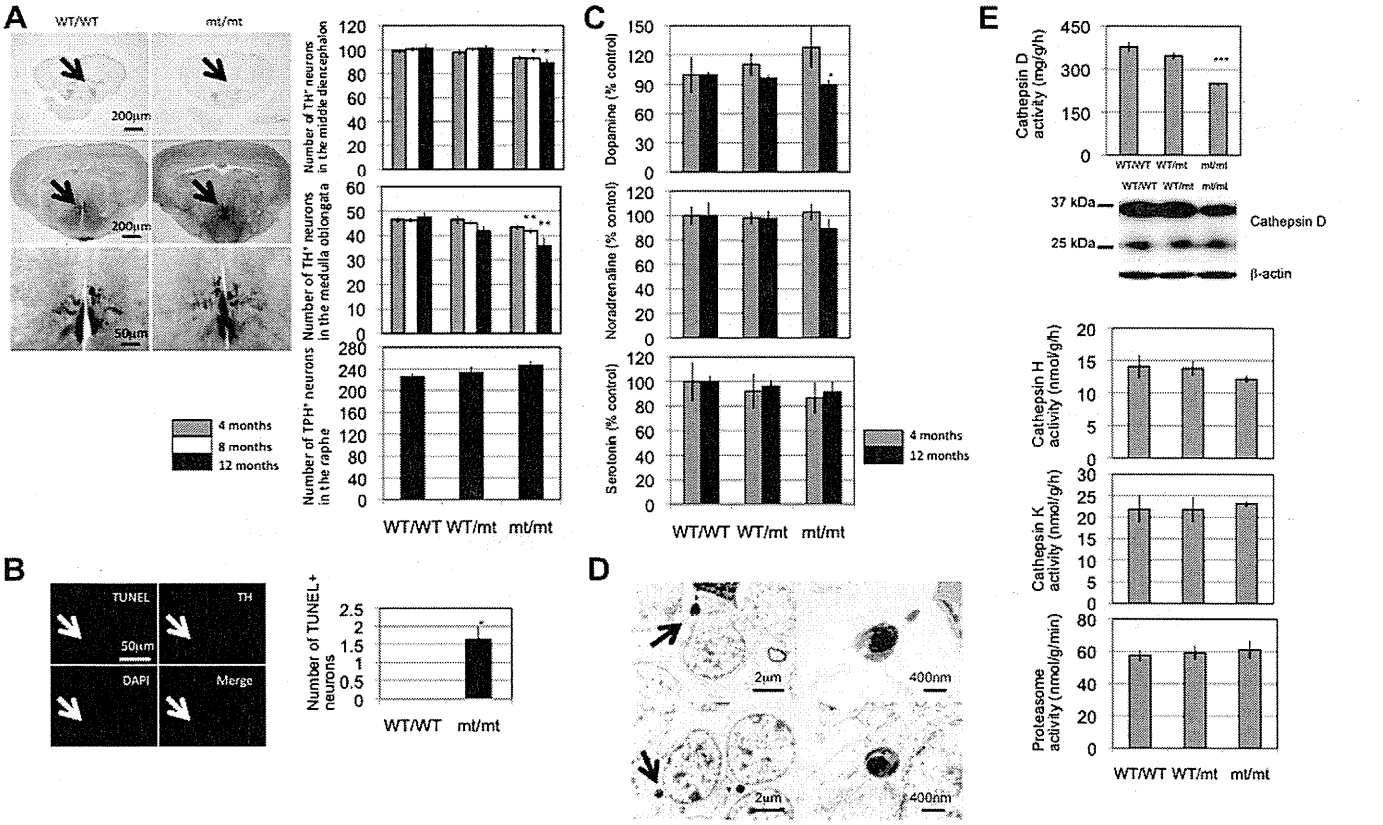

Fig. 5. Neuropathology of Atp13a2 mutant medaka. (A) Axial sections of telencephalon (upper) and middle diencephalon (middle and lower) of medaka brain at 12 months. Arrows indicate TH+ fibers and neurons. The lower figures are the enlarged image of middle figures. The graphs indicate the number of TH+ neurons in the middle diencephalon (upper) and medulla oblongata (middle) and the number of tryptophan-hydroxylase positive (TPH+) neurons in the raphe. $^{*}P < 0.05$ vs. WT/WT and WT/mt. $^{**}P < 0.01$ vs. WT/WT. ($n = 16$ for each group). Error bars, SEM. (B) TUNEL assay in medaka brain at 12 months. White arrow indicates one TUNEL/TH double positive neuron in the middle diencephalon of mt/mt fish. The graph shows the number of TH/TUNEL double positive neurons in the middle diencephalon ($n = 3$). $^{*}P < 0.05$ vs. WT/WT. (C) Amount of dopamine (upper), noradrenaline (middle), and serotonin (lower) in the brain of Atp13a2 mutant medaka. All values are expressed as a percentage of the amount (ng) per protein weight (mg) for WT/WT ($n = 8$ for each group). $^{*}P < 0.05$ vs. WT/WT. Error bars, S.E.M. (D) Fingerprint-like structures in Atp13a2 mutant medaka brain. Arrows indicate fingerprint-like structures in mt/mt brain. The right figures are the high magnification images of these structures. (E) Enzyme activity (Cathepsin D, H, K and proteasome activity) in the medaka brain. $^{***}P < 0.001$ vs. WT/T and WT/mt. Error bars, SEM. Image of a western blot shows cathepsin D protein in the medaka brain. Cross reactivity of the antibody against medaka cathepsin D is shown in the supplementary information (Fig. S5).

fatal neurogenerative disease in human and sheep [21,28–30]. Using electronmicroscopy, we also detected lysosome like body and granular deposits. Interestingly, we observed subcellular structures that resemble fingerprint-profile, and these structures resemble abnormal structures in the neurons of cathepsin D-deficient mice [15] and in human patients with neuronal ceroid lipofuscinosis [19–21] or with sphingolipidoses [31,32]. These results indicate that the primary cause of KRS/PARK9 is a lysosomal dysfunction and KRS/PARK9 could also be classified into a "lysosome disease".

We have recently used medaka fish to develop an animal model of PD [17,18,33,34]. Here, we found a mutation in our TILLING library that is almost identical to a PD-associated mutation in human patients. This medaka mutation results in the same abnormal splicing that is seen in the human patients with KRS/PARK9. Homozygous mutant fish exhibited selective loss of dopaminergic and noradrenergic neurons; this type of neuron loss is a pathology typically seen in human PD patients. Additionally, we found that tissues and cells in the brains from homozygous mutant medaka exhibited a specific reduction of cathepsin D protein and developed fingerprint-like subcellular structures. Both findings strongly indicate that the ATP13A2 mutation could lead to the dysfunction of lysosomes in medaka neurons.

Recently, Fonseca et al. injected Morpholinos against *atp13a2* into zebrafish embryo and showed that loss of Atp13a2 results in embryonic lethality [35]. As they also showed in zebrafish, *atp13a2* mRNA expressed not only in the brain but also in the entire body in medaka larvae (data not shown). This suggested that Atp13a2 is also important for some unknown function in other organs than the central nervous system. Our medaka model mimics the human mutation and showed pronounced reduction of *atp13a2* mRNA but not null expression. This might be helpful to study the long-term effect of Atp13a2 dysfunction.

As is the case of human patients with PD, cell death was specific to dopamine and noradrenaline neurons in our medaka model of KRS/ATP13A2. This cell-type specificity is also evident with our other medaka models of PD, including the models resulting from a lysosome inhibitor treatment [18,34]. The *atp13a2* mRNA, like other PD-related mRNAs, is expressed ubiquitously in the medaka brain [33]. Thus, the expression pattern of *atp13a2* could not explain the selective cell death in our model. Dopamine neurons contain toxic proteins derived from dopamine itself [36,37], and lysosomal function is essential in these neurons for preventing accumulation of the toxic proteins and other toxic metabolic products. Therefore, we speculate that dopamine neurons are especially vulnerable to lysosome dysfunction.

One negative finding is that mutant fish did not show slow locomotive movement, as do human PD patients. Based on our analysis, it seemed that the mutant fish swam the same amount, or more, than did control fish. In humans, loss of at least 80% of the dopaminergic neurons in substantia nigra seems necessary to evoke clear PD symptoms. The extent of the loss of dopaminergic

neurons in our medaka model might not be enough to evoke locomotive impairment. The mild increase of locomotion at 4 months seen in homozygous mutant might have a relation with the non-significant increase of dopamine at the same stage. Similar tentative increase of dopamine at younger stage is also observed in another PD model fish [33]. Such increased dopamine might harm the neurons, because the metabolism of dopamine is accompanied by the generation of oxidative radicals [38].

In conclusion, we demonstrated that reduction in ATP13A2 function in vitro or in vivo resulted in dysfunction of cathepsin D and the appearance of abnormal structures that are associated with lysosomal disorders. We used a teleost fish, medaka, to successfully generate an animal model suffered selective degeneration of dopaminergic neurons. Our findings indicate that lysosome-mediated autophagy may play a key role to protect dopaminergic neurons.

Acknowledgments

We wish to thank Kondoh Differentiation Signaling Project, JST, for permission to use the Kyoto-cab strain. We are grateful to Ai Tanigaki, Rie Hikawa and Junji Ezaki, who were very supportive of our experiments. We are also grateful to Satoshi Fukui, Mitsutaka Yoshida, Kaori Moriya, and Hidetake Kurihara for excellent assistance with our electron microscopy studies. This work was supported by JST-CREST. A part of this research was supported by a Grant-in-Aid for Young Scientists (B) (F. Sato) and a Grant-in-Aid for Scientific Research on Innovative Areas (Comprehensive Brain Science Network) (F. Sato) from the Ministry of Education, Science, Sports and Culture of Japan.

Appendix A. Supplementary data

Supplementary data associated with this article can be found, in the online version, at http://dx.doi.org/10.1016/j.febslet.2013.02.046.

References

[1] Gasser, T. (2007) Update on the genetics of Parkinson's disease. Mov. Disord. 22 (Suppl. 17), S343–S350.
[2] Najim al-Din, A.S., Wriekat, A., Mubaidin, A., Dasouki, M. and Hiari, M. (1994) Pallido-pyramidal degeneration, supranuclear upgaze paresis and dementia: Kufor-Rakeb syndrome. Acta Neurol. Scand. 89, 347–352.
[3] Ramirez, A., Heimbach, A., Gründemann, J., Stiller, B., Hampshire, D., Cid, L.P., Goebel, I., Mubaidin, A.F., Wriekat, A.L., Roeper, J., et al. (2006) Hereditary parkinsonism with dementia is caused by mutations in ATP13A2, encoding a lysosomal type 5 P-type ATPase. Nat. Genet. 38, 1184–1191.
[4] Di Fonzo, A., Chien, H.F., Socal, M., Giraudo, S., Tassorelli, C., Iliceto, G., Fabbrini, G., Marconi, R., Fincati, E., Abbruzzese, G., et al. (2007) ATP13A2 missense mutations in juvenile parkinsonism and young onset Parkinson disease. Neurology 68, 1557–1562.
[5] Ning, Y.P., Kanai, K., Tomiyama, H., Li, Y., Funayama, M., Yoshino, H., Sato, S., Asahina, M., Kuwabara, S., Takeda, A., et al. (2008) PARK9-linked parkinsonism in eastern Asia: mutation detection in ATP13A2 and clinical phenotype. Neurology 70, 1491–1493.
[6] Paisán-Ruiz, C., Guevara, R., Federoff, M., Hanagasi, H., Sina, F., Elahi, E., Schneider, S.A., Schwingenschuh, P., Bajaj, N., Emre, M., et al. (2010) Early-onset L-dopa-responsive parkinsonism with pyramidal signs due to ATP13A2, PLA2G6, FBXO7 and spatacsin mutations. Mov. Disord. 25, 1791–1800.
[7] Santoro, L., Breedveld, G.J., Manganelli, F., Iodice, R., Pisciotta, C., et al. (2011) Novel ATP13A2 (PARK9) homozygous mutation in a family with marked phenotype variability. Neurogenetics 12, 33–39.
[8] Crosiers, D., Ceulemans, B., Meeus, B., Nuytemans, K., Pals, P., Van Broeckhoven, C., Cras, P. and Theuns, J. (2011) Juvenile dystonia–parkinsonism and dementia caused by a novel ATP13A2 frame-shift mutation. Parkinsonism Relat. Disord. 17, 135–138.
[9] Lesage, S. and Brice, A. (2009) Parkinson's disease: from monogenic forms to genetic susceptibility factors. Hum. Mol. Genet. 18, R48–R59.
[10] Covy, J.P., Waxman, E.A. and Giasson, B.I. (2012) Characterization of cellular protective effects of ATP13A2/PARK9 expression and alterations resulting from pathogenic mutants. J. Neurosci. Res. 90, 2306–2316.
[11] Dehay, B., Ramirez, A., Martinez-Vicente, M., Perier, C., Canron, M.H., Doudnikoff, E., Vital, A., Vila, M., Klein, C. and Bezard, E.C. (2012) Loss of P-type ATPase ATP13A2/PARK9 function induces general lysosomal deficiency and leads to Parkinson disease neurodegeneration. Proc. Natl. Acad. Sci. USA 109, 9611–9616.
[12] Podhajska, A., Musso, A., Trancikova, A., Stafa, K., Moser, R., Sonnay, S., Glauser, L. and Moore, D.J. (2012) Common pathogenic effects of missense mutations in the P-type ATPase ATP13A2 (PARK9) associated with early-onset parkinsonism. PLoS ONE 7, e39942.
[13] Ramonet, D., Podhajska, A., Stafa, K., Sonnay, S., Trancikova, A., Tsika, E., Pletnikova, O., Troncoso, J.C., Glauser, L. and Moore, D.J. (2012) PARK9-associated ATP13A2 localizes to intracellular acidic vesicles and regulates cation homeostasis and neuronal integrity. Hum. Mol. Genet. 21, 1725–1743.
[14] Usenovic, M., Knight, A.L., Ray, A., Wong, V., Brown, K.R., Caldwell, G.A., Caldwell, K.A., Stagljar, I. and Krainc, D. (2012) Identification of novel ATP13A2 interactors and their role in α-synuclein misfolding and toxicity. Hum. Mol. Genet. 21, 3785–3794.
[15] Koike, M., Nakanishi, H., Saftig, P., Ezaki, J., Isahara, K., Ohsawa, Y., Schulz-Schaeffer, W., Watanabe, T., Waguri, S., Kametaka, S., et al. (2000) Cathepsin D deficiency induces lysosomal storage with ceroid lipofuscin in mouse CNS neurons. J. Neurosci. 20, 6898–6906.
[16] Taniguchi, Y., Takeda, S., Furutani-Seiki, M., Kamei, Y., Todo, T., Sasado, T., Deguchi, T., Kondoh, H., Mudde, J., Yamazoe, M., et al. (2006) Generation of medaka gene knockout models by target-selected mutagenesis. Genome Biol. 7, R116.
[17] Matsui, H., Taniguchi, Y., Inoue, H., Uemura, K., Takeda, S. and Takahashi, R. (2009) A chemical neurotoxin, MPTP induces Parkinson's disease like phenotype, movement disorders and persistent loss of dopamine neurons in medaka fish. Neurosci. Res. 65, 263–271.
[18] Matsui, H., Ito, H., Taniguchi, Y., Inoue, H., Takeda, S. and Takahashi, R. (2010) Proteasome inhibition in medaka brain induces the features of Parkinson's disease. J. Neurochem. 115, 178–187.
[19] Palmer, D.N., Fearnley, I.M., Walker, J.E., Hall, N.A., Lake, B.D., Wolfe, L.S., Haltia, M., Martinus, R.D. and Jolly, R.D. (1992) Mitochondrial ATP synthase subunit c storage in the ceroid-lipofuscinoses (Batten disease). Am. J. Med. Genet. 42, 561–567.
[20] Tsiakas, K., Steinfeld, R., Storch, S., Ezaki, J., Lukacs, Z., Kominami, E., Kohlschütter, A., Ullrich, K. and Braulke, T. (2004) Mutation of the glycosylated asparagine residue 286 in human CLN2 protein results in loss of enzymatic activity. Glycobiology 14, 1C–5C.
[21] Tyynelä, J., Palmer, D.N., Baumann, M. and Haltia, M. (1993) Storage of saposins A and D in infantile neuronal ceroid-lipofuscinosis. FEBS Lett. 330, 8–12.
[22] Spillantini, M.G., Schmidt, M.L., Lee, V.M., Trojanowski, J.Q., Jakes, R. and Goedert, M. (1997) Alpha-synuclein in Lewy bodies. Nature 388, 839–840.
[23] Webb, J.L., Ravikumar, B., Atkins, J., Skepper, J.N. and Rubinsztein, D.C. (2003) Alpha-synuclein is degraded by both autophagy and the proteasome. J. Biol. Chem. 278, 25009–25013.
[24] Narendra, D., Tanaka, A., Suen, D.F. and Youle, R.J. (2008) Parkin is recruited selectively to impaired mitochondria and promotes their autophagy. J. Cell Biol. 183, 795–803.
[25] Tan, J., Zhang, T., Jiang, L., Chi, J., Hu, D., Pan, Q., Wang, D. and Zhang, Z. (2011) Regulation of intracellular manganese homeostasis by Kufor-Rakeb syndrome-associated ATP13A2 protein. J. Biol. Chem. 286, 29654–29662.
[26] Sidransky, E., Nalls, M.A., Aasly, J.O., Aharon-Peretz, J., Annesi, G., Barbosa, E.R., Bar-Shira, A., Berg, D., Bras, J., Brice, A., et al. (2009) Multicenter analysis of glucocerebrosidase mutations in Parkinson's disease. N. Engl. J. Med. 361, 1651–1661.
[27] Usenovic, M., Tresse, E., Mazzulli, J.R., Taylor, J.P. and Krainc, D. (2012) Deficiency of ATP13A2 leads to lysosomal dysfunction, α-synuclein accumulation, and neurotoxicity. J. Neurosci. 32, 4240–4246.
[28] Siintola, E., Partanen, S., Strömme, P., Haapanen, A., Haltia, M., Maehlen, J., Lehesjoki, A.E. and Tyynelä, J. (2006) Cathepsin D deficiency underlies congenital human neuronal ceroid-lipofuscinosis. Brain 129, 1438–1445.
[29] Fritchie, K., Siintola, E., Armao, D., Lehesjoki, A.E., Marino, T., Powell, C., Tennison, M., Booker, J.M., Koch, S., Partanen, S., et al. (2009) Novel mutation and the first prenatal screening of cathepsin D deficiency (CLN10). Acta Neuropathol. 117, 201–208.
[30] Steinfeld, R., Reinhardt, K., Schreiber, K., Hillebrand, M., Kraetzner, R., Bruck, W., Saftig, P. and Gartner, J. (2006) Cathepsin D deficiency is associated with a human neurodegenerative disorder. Am. J. Hum. Genet. 78, 988–998.
[31] Jellinger, K., Anzil, A.P., Seemann, D. and Bernheimer, H. (1982) Adult GM2 gangliosidosis masquerading as slowly progressive muscular atrophy: motor neuron disease phenotype. Clin. Neuropathol. 1, 31–44.
[32] Idoate, M.A., Pardo-Mindan, F.J. and Gonzalez Alamillo, C. (1992) Fabry's disease without angiokeratomas showing unusual eccrine gland vacuolation. J. Pathol. 167, 65–68.
[33] Matsui, H., Taniguchi, Y., Inoue, H., Kobayashi, Y., Sakaki, Y., Toyoda, A., Uemura, K., Kobayashi, D., Takeda, S. and Takahashi, R. (2010) Loss of PINK1 in medaka fish (*Oryzias latipes*) causes late-onset decrease in spontaneous movement. Neurosci. Res. 66, 151–161.
[34] Matsui, H., Ito, H., Taniguchi, Y., Takeda, S. and Takahashi, R. (2010) Ammonium chloride and tunicamycin are novel toxins for dopaminergic neurons and induce Parkinson's disease-like phenotypes in medaka fish. J. Neurochem. 115, 1150–1160.

[35] Lopes da Fonseca, T., Correia, A., Hasselaar, W., van der Linde, H.C., Willemsen, R. and Outeiro, T.F. (2013) The zebrafish homologue of Parkinson's disease ATP13A2 is essential for embryonic survival. Brain Res. Bull. 90, 118–126.
[36] Barzilai, A., Daily, D., Zilkha-Falb, R., Ziv, I., Offen, D., Melamed, E. and Shirvan, A. (2003) The molecular mechanisms of dopamine toxicity. Adv. Neurol. 91, 73–82.
[37] Gandhi, S., Vaarmann, A., Yao, Z., Duchen, M.R., Wood, N.W. and Abramov, A.Y. (2012) Dopamine induced neurodegeneration in a PINK1 model of Parkinson's disease. PLoS ONE 7, e37564.
[38] Blum, D., Torch, S., Lambeng, N., Nissou, M., Benabid, A.L., Sadoul, R. and Verna, J.M. (2001) Molecular pathways involved in the neurotoxicity of 6-OHDA, dopamine and MPTP: contribution to the apoptotic theory in Parkinson's disease. Prog. Neurobiol. 65, 135–172.

Parkinsonism and Related Disorders 19 (2013) 15–20

Contents lists available at SciVerse ScienceDirect

Parkinsonism and Related Disorders

journal homepage: www.elsevier.com/locate/parkreldis

Analyses of the *MAPT*, *PGRN*, and *C9orf72* mutations in Japanese patients with FTLD, PSP, and CBS

Kotaro Ogaki [a], Yuanzhe Li [b], Masashi Takanashi [a], Kei-Ichi Ishikawa [a], Tomonori Kobayashi [d], Takashi Nonaka [e], Masato Hasegawa [e], Masahiko Kishi [f], Hiroyo Yoshino [b], Manabu Funayama [a,b], Tetsuro Tsukamoto [g], Keiichi Shioya [h], Masayuki Yokochi [i], Hisamasa Imai [a], Ryogen Sasaki [j], Yasumasa Kokubo [j], Shigeki Kuzuhara [k], Yumiko Motoi [a], Hiroyuki Tomiyama [a,c], Nobutaka Hattori [a,b,c,*]

[a] *Department of Neurology, Juntendo University School of Medicine, Tokyo, Japan*
[b] *Research Institute for Diseases of Old Age, Juntendo University School of Medicine, Tokyo, Japan*
[c] *Department of Neuroscience for Neurodegenerative Disorders, Juntendo University School of Medicine, Tokyo, Japan*
[d] *Department of Neurology, Fukuoka University School of Medicine, Fukuoka, Japan*
[e] *Department of Neuropathology and Cell Biology, Tokyo Metropolitan Institute of Medical Science, Tokyo, Japan*
[f] *Department of Internal Medicine, Division of Neurology, Sakura Medical Center, Toho University, Sakura, Japan*
[g] *Department of Neurology, Numazu Rehabilitation Hospital, Numazu, Japan*
[h] *Department of Neurology, National Hospital Organization Miyazaki Higashi Hospital, Miyazaki, Japan*
[i] *Department of Neurology, Tokyo Metropolitan Health and Medical Treatment Corp., Ebara Hospital, Tokyo, Japan*
[j] *Department of Neurology, Mie University Graduate School of Medicine, Tsu, Mie, Japan*
[k] *Department of Medical Welfare, Faculty of Health Science, Suzuka University of Medical Science, Suzuka, Mie, Japan*

ARTICLE INFO

Article history:
Received 26 April 2012
Received in revised form
16 June 2012
Accepted 19 June 2012

Keywords:
MAPT
PGRN
C9orf72
De novo
Abnormal eye movements

ABSTRACT

Background: Mutations in the microtubule associated protein tau (*MAPT*) and progranulin (*PGRN*) have been identified in several neurodegenerative disorders, such as frontotemporal lobar degeneration (FTLD), progressive supranuclear palsy (PSP), and corticobasal syndrome (CBS). Recently, *C9orf72* repeat expansion was reported to cause FTLD and amyotrophic lateral sclerosis (ALS). To date, no comprehensive analyses of mutations in these three genes have been performed in Asian populations. The aim of this study was to investigate the genetic and clinical features of Japanese patients with *MAPT*, *PGRN*, or *C9orf72* mutations.

Methods: *MAPT* and *PGRN* were analyzed by direct sequencing and gene dosage assays, and *C9orf72* repeat expansion was analyzed by repeat-primed PCR in 75 (48 familial, 27 sporadic) Japanese patients with FTLD, PSP, or CBS.

Results: We found four *MAPT* mutations in six families, one novel *PGRN* deletion/insertion, and no repeat expansion in *C9orf72*. Intriguingly, we identified a *de novo* *MAPT* p.S285R mutation. All six patients with early-onset PSP and the abnormal eye movements that are not typical of sporadic PSP had *MAPT* mutations. The gene dosages of *MAPT* and *PGRN* were normal.

Discussion: *MAPT* p.S285R is the first reported *de novo* mutation in a sporadic adult-onset patient. *MAPT* mutation analysis is recommended in both familial and sporadic patients, especially in early-onset PSP patients with these abnormal eye movements. Although *PGRN* and *C9orf72* mutations were rare in this study, the *PGRN* mutation was found in this Asian FTLD. These genes should be studied further to improve the clinicogenetic diagnoses of FTLD, PSP, and CBS.

1. Introduction

Mutations in the microtubule-associated protein tau (*MAPT*) and the progranulin (*PGRN*) genes have been identified in families with frontotemporal dementia and parkinsonism linked to chromosome 17 [1–3]. Recently, two studies reported that the expansion of a noncoding GGGGCC hexanucleotide repeat in the *C9orf72* gene is

* Corresponding author. Department of Neurology, Juntendo University School of Medicine, 2-1-1 Hongo, Bunkyo, Tokyo 113-8421, Japan. Tel.: +81 3 5802 1073; fax: +81 3 5800 0547.
E-mail address: nhattori@juntendo.ac.jp (N. Hattori).

1353-8020/$ – see front matter © 2012 Published by Elsevier Ltd.
http://dx.doi.org/10.1016/j.parkreldis.2012.06.019

a major cause of both frontotemporal lobar degeneration (FTLD) and amyotrophic lateral sclerosis (ALS) [4,5].

Each of these genes can be associated with multiple clinical entities. Patients with *MAPT* mutations may receive diagnoses of frontotemporal dementia (FTD), primary progressive aphasia (PPA), or progressive supranuclear palsy (PSP). Rarely, corticobasal syndrome (CBS) or FTD with ALS (FTD-ALS) may be manifested in these patients [6]. The clinical diagnoses of patients with *PGRN* mutations include FTD, PPA, and CBS [6]. *C9orf72* repeat expansion causes FTD, ALS, FTD-ALS [4,5], PPA [5,7], and CBS [8] phenotypes. Thus, due to the complicated and often overlapping genetic and phenotypic variability in these patients, an accurate diagnosis of these clinical entities before autopsy is often difficult for clinicians.

To date, few comprehensive screening studies of these three genes have been performed in Asian populations. The aims of this study are to characterize the roles of known and, more importantly, novel disease-causing genes and to investigate the genetic and clinical features of FTLD, PSP, and CBS patients with *MAPT*, *PGRN*, and *C9orf72* mutations. In this study, we also describe the abnormal eye movements that are generally not observed in sporadic PSP but occur in early-onset PSP patients bearing *MAPT* mutations.

2. Methods

2.1. Subjects

We studied 75 Japanese patients who were diagnosed with FTLD, PSP, and CBS with or without a family history of disease. FTLD was divided into three subclasses: behavioral variant FTD (bvFTD), FTD-ALS, and PPA. The clinical diagnoses were established according to the consensus criteria for FTD [9], PPA [10], PSP [11], and CBS [12]. The characteristics of the 75 analyzed patients (69 index patients) are shown in Table 1. This study was approved by the ethics committee of the Juntendo University School of Medicine. Each subject provided written informed consent. All of the subjects in the control cohort were Japanese individuals and were evaluated by neurologists to ensure that no subjects exhibited any clinical manifestations of neurodegenerative diseases.

2.2. Genetic analyses

For direct sequence analysis, each exon was amplified by polymerase chain reaction (PCR) using published primers for *MAPT* [13] and *PGRN* [2] in a standard protocol. Dideoxy cycle sequencing was performed using Big Dye Terminator chemistry (Applied Biosystems, Foster City, CA). These products were loaded into ABI310 and 3130 automated DNA sequence analyzers and analyzed with DNA Sequence Analysis software (Applied Biosystems). To provide a qualitative assessment of the presence of an expanded $(GGGGCC)_n$ hexanucleotide repeat in the *C9orf72* gene, we performed repeat-primed PCR as previously described [4]. The normal repeat number of the GGGGCC hexanucleotide was determined in all of the patients using genotyping primers, as previously described [4]. The PCR products were analyzed on an ABI3130 DNA Analyzer and visualized using Gene Mapper software (Applied Biosystems).

Table 1
The clinical diagnoses and characteristics of 75 patients (69 index patients).

Clinical phenotype	No.	% of total	% of Male	Mean (SD) AAO (range, years)	Familial	Sporadic
FTLD	38	50.7	39.5	57.1 (±12.4), 36–78	21	17
bvFTD	29	38.7	34.5	54.5 (±12.6), 36–78	18	11
FTD-ALS	2	2.7	100	67.5 (±1.5), 66–69	1	1
PPA	7	9.3	42.9	65.0 (±7.4), 58–77	2	5
PSP	25	33.3	68.0	59.8 (±13.0), 40–76	18	7
CBS	12	16.0	33.3	58.4 (±9.52), 40–71	9	3
Total	75	100	48.0	58.2 (±12.3), 36–78	48	27
Index patients	69	92.0	46.4	58.9 (±12.4), 36–78	42	27
Relatives	6	8	66.7	50.3 (±6.6), 44–61	6	0

FTLD = frontotemporal lobar degeneration.
bvFTD = behavioral variant frontotemporal dementia.
FTD-ALS = frontotemporal dementia with amyotrophic lateral sclerosis.
PPA = primary progressive aphasia; PSP = progressive supranuclear palsy.
CBS = corticobasal syndrome; SD = standard deviation; AAO = age at onset.

2.3. Multiplex ligation-dependent probe amplification (MLPA)

To confirm the gene dosages of *MAPT* and *PGRN*, we performed MLPA using the SALSA MLPA P275-B1 MAPT-PGRN kit (MRC-Holland, Amsterdam, The Netherlands). The DNA detection/quantification protocol was provided by the manufacturer. The products were quantified using the ABI3130 Genetic Analyzer and Gene Mapper v3.7 (Applied Biosystems). The kit contains 32 probes, including 13 *MAPT* probes (located in exons 1–13) and 5 *PGRN* probes (located in exons 1, 3, 6, 10, and 12) located within other genes on chromosome 17q21. The MLPA data were analyzed as described previously [14].

2.4. Exon-trapping analysis

To determine whether a novel *MAPT* mutation was pathogenic, we performed an exon-trapping analysis. We used a wild-type construct and constructs containing the novel *MAPT* p.S285R or the IVS10+3 intronic mutation [15]. The *MAPT* sequences included exon 10, 34 nucleotides of the upstream intronic sequence and 85 nucleotides of the downstream intronic sequence. The PCR products were subcloned into the splicing vector pSPL3 (Invitrogen, Carlsbad, CA), and exon trapping was performed as described previously [15].

2.5. Paternity testing

Microsatellite analysis with 10 markers (D2S293, D3S3521, D4S2971, D5S495, D6S16171, D7S2459, D8S1705, D16S430, D18S450, and D20S842) was performed in Patient 1 and his parents to confirm paternity.

2.6. TA cloning

The novel *PGRN* heterozygous deletion/insertion found in this study, *PGRN* p.G338RfsX23 (c.1012_1013delGGinsC), was confirmed by cloning the PCR products into the pCR4-TOPO Vector using the TOPO TA Cloning kit (Invitrogen) and sequencing the two haplotypes of the heterozygote.

3. Results

3.1. Results of MAPT analysis

3.1.1. Genetic and molecular analyses of MAPT

In this study, we identified nine patients with *MAPT* mutations from six families. Four heterozygous missense mutations in *MAPT*, p.L266V, p.N279K, p.N296N, and the novel p.S285R (Supplementary Fig. 1), were identified by direct sequencing. None of the 182 normal Japanese controls included in this study had the *MAPT* p.S285R. In addition, we examined the amino acid sequences of the MAPT protein in other species and found that the site of the p.S285R mutation was highly conserved (see Supplementary Fig. 2). The novel p.S285R mutation in *MAPT* was detected in Patient 1 but not in his parents (Fig. 1A and Supplementary Fig. 1). The parentage of this patient and the DNA authenticity were confirmed using a microsatellite panel (see Supplementary Table 1). These results suggest that p.S285R is a *de novo* mutation. To investigate whether the p.S285R mutation is pathogenic, we performed an exon-trapping analysis. The p.S285R mutation produced a marked increase in the splicing of exon 10 (Fig. 1B) and resulted in the overproduction of tau isoforms that contain 4-repeat tau, such as IVS10+3 [15]. These results indicate that the p.S285R mutation is a novel, *de novo* pathogenic mutation. Previously, p.L266V, p.N279K, and p.N296N had been reported as pathogenic mutations [16–18].

Table 2 lists the clinical features of all of the *MAPT*- and *PGRN*-positive patients in this study, and Supplementary Fig. 3 shows Pedigrees C, D, E, F, and G. The average age at disease onset of patients with a single heterozygous *MAPT* mutation was 42.3 ± 2.9 (range: 37–46) years. MLPA analysis showed no gene dosage abnormalities (multiplications or deletions) in *MAPT* in this cohort.

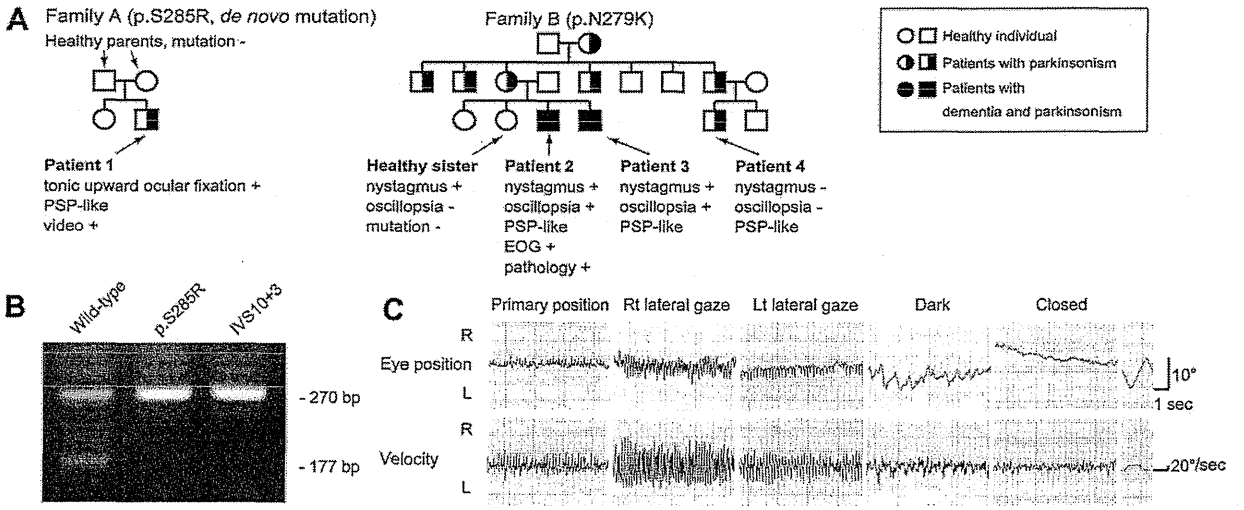

Fig. 1. (A) The pedigrees of families A and B. (B) Exon-trapping analysis for the effects of the *MAPT* p.S285R mutation on exon 10 splicing. (C) Horizontal electro-oculogram recordings in Patient 2.

3.1.2. Clinical presentations of MAPT-positive patients with the abnormal eye movements that are generally not observed in patients with sporadic PSP

3.1.2.1. Patient 1 (MAPT p.S285R). This patient was a 46-year-old man who presented with difficulty speaking and breathing. The patient had no family history of dementia or movement disorders (Fig. 1A). A physical examination revealed gait disturbance, limb bradykinesia, and frequent falling. At age 47, the patient exhibited palilalia and a mild obsession with eating. The patient's Mini-Mental State Examination (MMSE) score was 28/30, but his Frontal Assessment Battery score was 12/18. The patient exhibited a slowing of saccadic eye movements with a relative preservation of smooth pursuit, vertical supranuclear gaze palsy, and tonic upward ocular fixation (see Video Supplement); when the patient's eyes opened after closing, they remained fixated upward and could not be moved voluntarily to the primary position (i.e., Bell's phenomenon remained). To overcome this disability, the patient extended his neck, which resulted in a reflex downward movement of the eyes (the vestibulo-ocular reflex), and next he slightly flexed his neck to a neutral position with his eyes in the primary position. Later, the patient developed bradykinesia and postural instability with frequent falling. L-dopa/benserazide (up to 900 mg/day) was ineffective. The patient's condition gradually deteriorated, and he developed dementia, retrocollis, vertical and horizontal supranuclear palsy, and bradykinesia. At age 49, the patient died of suffocation from the aspiration of food material. No autopsy was performed. The clinical diagnosis was probable PSP.

3.1.2.2. Patient 2 (MAPT p.N279K). This patient was the older brother of Patient 3 (Fig. 1A). Patient 2 was a 42-year-old man who exhibited oscillopsia, micrographia, and a shuffling gait. This patient reported having had nystagmus without oscillopsia since childhood. A neurological examination revealed marked horizontal nystagmus. The patient's pupils were isocoric, and his visual acuity was normal. The patient presented with rigidity, bradykinesia, and postural tremor in the upper limbs. Electro-oculography revealed horizontal pendular nystagmus in the primary position and in all gaze directions (Fig. 1C). L-dopa/benserazide at 200 mg/day mildly alleviated his parkinsonism. Two years later, the patient developed prominent postural instability and became prone to falling. Upward and downward gaze palsy and apraxia of eyelid opening were also noted. At that time, the clinical diagnosis was possible PSP with a family history of dementia and parkinsonism. The patient's cognitive function deteriorated gradually. At age 52, he was bedridden and required a gastrostomy. The patient died of pneumonia at age 54. A postmortem pathological examination of the brain revealed mild atrophy of the frontal lobe and the tegmentum of the midbrain and pons. Microscopic analysis showed severe degenerative changes in the substantia nigra and the subcortical nuclei. Immunohistochemistry using anti-phosphorylated tau (p-tau) antibodies revealed numerous tau-positive neuronal and glial inclusions in the frontotemporal cortex, white matter, and the subcortical nuclei (see Supplementary Fig. 4). These p-tau deposits reacted with anti-4-repeat tau antibodies but not with anti-3-repeat tau antibodies.

3.1.2.3. Patient 3 (MAPT p.N279K). This patient was the younger brother of Patient 2 (Fig. 1A). At age 44, Patient 3 noticed clumsiness in his right hand and oscillopsia. The patient reported having nystagmus since childhood. A neurological examination revealed large, horizontal pendular nystagmus in the primary position and in all gaze directions. The patient's visual acuity, pupils, and light reflexes were all normal. Mild bradykinesia and rigidity in the neck and the right upper limb were noted. Postural tremor in both hands and the tongue and postural instability were observed. Treatment with 600 mg/day of L-dopa/carbidopa was not effective. The patient's oscillopsia gradually worsened, and eventually he was unable to read printed materials. At age 47, the patient developed upward and downward gaze palsy, slowing of saccades, and apraxia of eyelid opening. The patient had prominent postural instability and was prone to falling. The patient's first clinical diagnosis was possible PSP with a family history of dementia and parkinsonism. The patient died at age 56. An autopsy was not performed.

3.1.2.4. Patients 5, 6, and 7 (MAPT p.N279K). The clinical presentations of these three patients have been described previously [19]. All three patients had clinical diagnoses of possible PSP (Table 2) and visual grasping [19,20].

3.2. Results of PGRN analysis

3.2.1. Genetic Analyses of PGRN

We identified one patient with a *PGRN* mutation (Table 2, Supplementary Fig. 3). One novel heterozygous deletion/insertion

Table 2
Clinical features of patients with *MAPT* and *PGRN* mutations.

Family	A	B			C	D		E	F	G
Patient	1	2	3	4	5	6	7	8	9	10
Gene					*MAPT*					*PGRN*
Genotyping					Heterozygous					
Nucleotide change	c.853A > C	c.837T > G	c.837T > G	c.837T > G	c.837T > G	c.837T > G	c.837T > G	c.796C > G	c.888T > C	c.1012_1013delGGinsC
Amino acid change	p.S285R	p.N279K	p.N279K	p.N279K	p.N279K	p.N279K	p.N279K	p.L266V	p.N296N	p.G338RfsX23
Exon	10	10	10	10	10	10	10	9	10	9
Mode of inheritance	*de novo*	AD	AD	AD	NA	AD	AD	AD	AD	AD
Age at onset, years	46	42	44	46	41	42	43	37	44	59
Age at evaluation, years	47	47	45	50	44	44	45	38	49	61
Age at death, years	49	54	56	alive	51	54	51	alive	alive	alive
Sex	M	M	M	M	F	F	F	F	M	F
Clinical syndromes	PSP	PSP	PSP	PSP	PSP	PSP	PSP	bvFTD	PSP	PPA
Clinical features										
Initial symptoms	P	P	P	P	P	P	P	dementia	P	aphasia
Personality/behavior changes	−	+	−	−	−	−	−	+	+	−
Mini mental state examination score	28/30	NA	NA	28/30	NA	NA	NA	0	24/30	29/30
Hasegawa dementia scale-revised[a]	NA	18/30	NA	NA	21/30	28/30	30/30	0	21/30	29/30
Nonfluent spontaneous speech	−	−	−	−	−	−	−	−	−	+
Apraxia of eyelid opening	−	+	+	+	+	+	+	−	−	−
Abnormal eye movements										
Supranuclear gaze palsy	+	+	+	+	+	+	+	−	+	−
Tonic upward ocular fixation	+	−	−	−	−	−	−	−	−	−
Oscillopsia with CN	−	+	+	−	−	−	−	−	−	−
Visual grasping	−	−	−	−	+	+	+	−	−	−
Parkinsonism										
Bradykinesia	+	+	+	+	+	+	+	−	+	−
Rigidity	−	+	+	+	+	+	+	−	+	−
Tremor	−	+	+	−	−	−	−	−	−	−
Postural instability	+	+	+	+	+	+	+	−	+	−
Response to L-dopa	−	partial[b]	−	partial[b]	partial[b]	partial[b]	partial[b]	NA	+	NA
Pyramidal sign	+	−	NA	−	+	−	+	+	+	−
Features of motor neuron disease	−	−	−	−	−	−	−	−	−	−
Reference					[19]	[19]	[19]			

AD = autosomal dominant.
P = parkinsonism; NA = not available.
CN = congenital nystagmus; PSP = progressive supranuclear palsy.
bvFTD = behavioral variant frontotemporal dementia; PPA = primary progressive aphasia.
[a] The Hasegawa dementia scale-revised is a brief dementia screening scale. The maximum score of the Hasegawa dementia scale-revised is 30 points. There was a significant difference in the mean score between the demented and non-demented subjects when the cut-off point was set at 20/21 [31].
[b] A partial response to L-dopa indicates that L-dopa was effective only in the early stages.

mutation in *PGRN*, p.G338RfsX23 (c.1012_1013delGGinsC), was detected by direct sequencing and TOPO TA cloning sequencing (Supplementary Fig. 1). None of the 182 normal Japanese controls included in this study had the *PGRN* p.G338RfsX23 (c.1012_1013delGGinsC) mutations. The age at disease onset of the patient with the heterozygous *PGRN* deletion/insertion was 59 years. Novel *PGRN* variants with unknown significance, p.R18Q and p.N118del, are listed in Table 3. MLPA analysis showed no gene dosage abnormalities in *PGRN*.

3.2.2. A clinical presentation of a novel PGRN mutation
3.2.2.1. Patient 10 (PGRN p.G338RfsX23, c.1012_1013delGGinsC). This patient, a 59-year-old woman, developed word-finding difficulties and underwent surgical clipping at age 54 for an unruptured

Table 3
Novel variants with unknown significance.

Gene	Nucleotidechange	Amino acid change	Exon	Amino acid conservation	Mean AAO (years)	Frequency		*P* value	Clinical diagnosis
						Patients *N* (%)	Controls *N* (%)		
PGRN	c.56G > A	p.R19Q	1	not conserved	66	1/69 (1.4)	0/186 (0)	0.605	PSP ($n = 1$)
PGRN	c.352_354delAAC	p.N118del	4	not conserved	53	3/69 (4.3)	3/272 (1.1)	0.187	bvFTD ($n = 3$)

AAO = age at onset.
PSP = progressive supranuclear palsy.
bvFTD = behavioral variant frontotemporal dementia.